# Optimal Design of a Fault-Tolerant IPM Motor with High Torque Density for Electric Power Steering System

HAMIDREZA AKHONDI BABAK ABDI
Electrical Engineering Department
Damavand Islamic Azad University
Beheshti Blvd, Damavand, Tehran.
IRAN
hamidreza9595@gmail.com

*Abstract:* - Electric Power Steering system provides the assist steer torque in vehicle through an electric motor. Since the electric motor is directly connected to the mechanical steering rack, must have the following features: Torque production with minimum Ripple for Precise steer control, High efficiency, easy Manufacturing technology and minimum size and weight. Motor structure optimization is done in order to increasing force to motor volume ratio, increasing fault tolerance, decreasing Permanent Magnet volume and force ripple. In this paper, Analytical relations Necessary and relevant for optimization have been obtained and finally desired objective function is defined in terms of machine design parameters such as air gap length, inner and outer machine diameter, slots dimensions, PM dimensions and location and machine electric and magnetic characteristics. Motor behavior study and confirmation in force production with determined power supply is done with finite element method simulation. At the end, entire electric power steering system including electric motor, power supply and controller have been simulated and the performance evaluation of system is done.

*Key-Words:* - Electric Power Steering-Optimization-Finite Element Method-Fault Tolerance-Torque Ripple

## 1 Introduction

The effects of global warming are becoming increasingly apparent. As a result, we product engineers are being asked to develop products that are friendlier to the earth's environment. Electric power steering (EPS) is such a product. By using power only when the steering wheel is turned by the driver, it consumes approximately one twentieth the energy of conventional hydraulic power steering systems and, as it does not contain any oil, it does not pollute the environment both when it is produced and discarded. While offering these environmental benefits now, in the future EPS is expected to facilitate automatic steering user-friendly technology that should ultimately reduce traffic accidents. Additionally, the software built into the EPS controller results in high performance and easy tuning during the development of prototypes of EPS systems. Because of these advantages, EPS has drawn the attention of automobile manufacturers all over the world.

Every movement requires energy. This is why Electric Power Steering only acts when it is needed. To give more bends per liter, an electric motor is used to assist the steering. However, unlike conventional hydraulic systems, Electric Power Steering is supported by an electric motor which helps to ensure that energy is only used during actual steering maneuvers. If the steering wheel is kept in a constant position when driving straight ahead or cornering, the electric motor is inactive and therefore does not use any energy.

The EPS system consists of a torque sensor, which senses the driver's movements of the steering wheel as well as the movement of the vehicle; an ECU, which performs calculations on assisting force based on signals from the torque and vehicle speed sensor; a motor, which produces turning force according to output from the ECU; and a reduction gear, which increases the turning force from the motor and transfers it to the steering mechanism. EPS is available in three types: a column type in which the reduction gear is located directly under the steering wheel, a pinion type in which the reduction gear is attached to the pinion of the rack and pinion assembly, and a rack type in which the reduction gear is installed to the rack. Each type of EPS system is speed sensitive that means the vehicle speed and engine rotation signals are input from the vehicle into the ECU [1].

The motor for EPS is an interior permanent magnetic synchronous motor (IPM). Attached to the

power steering gear assembly, it generates steering assisting force. This motor in EPS system must have the following operating requirements:

• The motor must be able to generate torque without turning.

• The motor must be able to reverse its rotation abruptly.

• The fact that motor vibration and torque fluctuations are directly transferred through the steering wheel to the hands of the driver must be considered.

The IPM motor presents many advantages over the other motors. Among them, it exhibits following features:

• Small, lightweight and high-output and efficiency
• Small fluctuations in torque during operation
• Low vibration and noise
• Low inertia and Low friction torque
• Flux weakening operation capability
• High torque density

The PSM offers higher efficiency, smaller space requirements and lower weight. They thus make an additional contribution to reductions in consumption and emissions.

The fault tolerance for IPM motors is necessary for optimization. Also the ability of design electric motor with high torque density and low torque pulsation is critical for applications of IPM for hybrid electric vehicles.

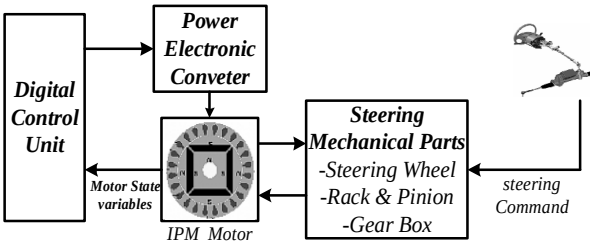


Fig. 1. Block Diagram of Overall EPS System

In this paper two items will be deeply analyzed. First, fault tolerant capability is an imperative requirement to the electric motor for steering application: In fact, a motor fault may cause a hard or impossible steer of the vehicle. For the sake of fault-tolerant capability, the IPM motor has to be able to satisfy severe operational constraints. Second, the torque density of IPM motor that considered in the optimization process. The components of system such IPMSM electrical and mechanical parts, power electronic converter, steering mechanism and controller are integrated as entire model of EPS using Simulink environment for analyzing the system performance with interactions between each component. The block diagram of EPS with IPMSM drive system is shown in Fig. 1.

## 2 Electric motor specifications in EPS

In the case of Electric Power Steering, a sensor registers the driver's steering movements and electronically controls an electric motor on the steering column or the steering rack. This generates a torque sufficient to the requirements, which supports the driver's steering movement.

In terms of the ability to withstand crashes (particularly secondary impacts), pinion-type EPS has an advantage over the column-type and rack-type in that the impact absorbing columns currently in use can be used as they are. Pinion-type EPS, like the column-type and rack-type EPS, consists of a torque sensor, reduction gear, motor, rack and pinion. The auxiliary power of the motor is directly transferred to the pinion shaft. The pinion-type gear assembly is located in the engine compartment so it is made very durable to enable it to endure the heat from the engine as well as water from outside the vehicle. The ECU, on the other hand, is located in the vehicle interior and is therefore free from the influence of heat and water. To help make the system lightweight and compact, the motor is small and the reduction gear has only one stage [2]. Pinion-type EPS is available in various sizes for different motor outputs from 25A to 60A. The pinion-type EPS system was developed for small cars. Its main specifications are listed in Table 1.

Table 1. Technical specifications of pinion-type EPS

| | | |
|---|---|---|
| Motor | Interior Permanent Magnet Synchronous Motor | |
| | Rated Speed | 1245 RPM |
| | Rated Torque | 3.7 N.m |
| | Rated Current | 42A |
| Controller | • Active return to center for steering wheel<br>• Active damper for vehicle stability enhancement<br>• Differential compensation<br>• Friction compensation | |
| | Control range of motor current | 0-42A |
| | Rated voltage | 12V DC |
| Torque sensor | Non-contact self-induction | |
| | Rated voltage | 12V DC |
| Reduction gear | Plastic worm and worm wheel | |
| | Reduction ratio | 15:1 |
| Gear specification | Stroke ratio | 40 mm/rev |
| | Rack ratio | 136 mm |
| | Lock to lock steering wheel | 3.4 rev |
| Maximum rack thrust | | 4.75 kN |

## 3 Design a fault tolerant IPM motor

Fault-tolerant design refers to a method for designing a system so it will continue to operate, possibly at a reduced level also known as graceful degradation, rather than failing completely, when some part of the system fails. That is, the system as a whole is not stopped due to problems either in the hardware or the software. There are many faults that may occur on the motor and electric drive such as short circuit and power electronic switches malfunction [1]. Component failures that would cause loss of steering capability with the basic architecture of the electrical steering system are listed in table 2. The more dangerous condition is considered the three-phase short circuit. Because of the PM flux linkage, the IPM motor works as an electric brake, so motor braking torque limits the steering movement. Thus it is necessary to reduce maximum braking torque under at least 10% rated torque.

Table 2. Critical EPS component failures

| subsystem | component | type of failure |
|---|---|---|
| drive | gate-driver<br>switch<br>switch | malfunction<br>short circuit<br>fail open |
| motor | winding<br>winding<br>harness<br>harness<br>bearing | open phase<br>turn short<br>open phase<br>phase to ground<br>stuck |
| sensor | DC link<br>voltage | malfunction<br>malfunction |
| power | harness | low |

In order to minimizing braking torque we have to obtain the IPM motor braking torque in case of three phase short circuit [4]. The analysis of the three phase short circuit and steady-state braking torque is carried out in the synchronous $d-q$ reference frame. The voltage equations are expressed by the following equations:

$$v_d = R_s i_d + \frac{d\, l_d}{dt} - w\, l_q$$
$$v_q = R_s i_q + \frac{d\, l_q}{dt} - w\, l_d \quad (1)$$

In the assumption of magnetic linearity, the $d$ and $q$-axis flux linkages are:

$$l_d = L_d i_d + l_m \;\;,\;\; l_q = L_q i_q \quad (2)$$

For the steady state study the equation (1) is without derivatives and with $v_d = v_q = 0$. The steady-state short circuit currents result in:

$$i_{d_{sc}} = -\frac{w^2 L_q\, l_m}{R_s^2 + w^2 L_d L_q}$$
$$i_{q_{sc}} = -\frac{w R_s\, l_m}{R_s^2 + w^2 L_d L_q} \quad (3)$$

Fig. 2 shows *id* and *iq* versus time. Final values of currents in this case of simulation have been determined on figure. Also Fig. 3 shows the $i_d$ and $i_q$ currents in the ($i_d$, $i_q$) plane. The IPM motor electrical parameters are given in table 3. The dashed line represents the ellipse trajectory described by the currents when the stator resistance is zero. Also, the solid line refers to the case with a resistance different from zero. The currents move from their initial value given by the operating point before the fault (and highlighted by the circle in Fig. 4) toward the steady-state short circuit value, which is defined by the equation (3). The initial values of currents used for simulation are $I_{d0} = -29.4$ A and $I_{q0} = 35.7$ A.

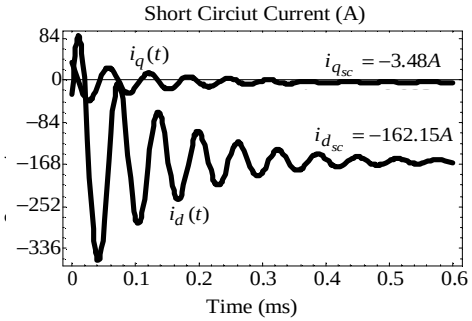


Fig. 2. Motor short circuit currents

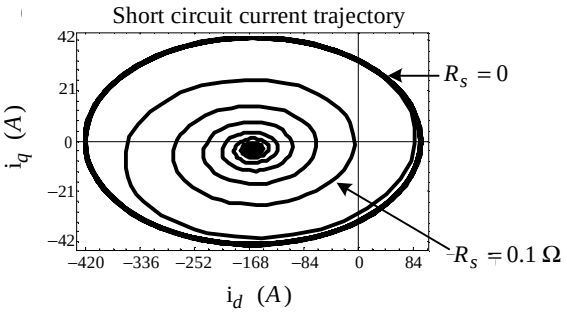


Fig. 3. $i_d$ and $i_q$ currents in the ($i_d$, $i_q$)

The minimum $d$-axis current is important, since it represents the peak negative current that may demagnetize the PMs. Consequently, the IPM motor has to be designed so as to sustain this current. It is computed as:

$$I_{d\min} = -\frac{l_m}{L_d} - \sqrt{\left(I_{d0} + \frac{l_m}{L_d}\right)^2 + \left(\frac{L_q}{L_d} I_{q0}\right)^2} \quad (4)$$

In this simulation, $I_{dmin} = -369.6$ A. Its amplitude is

about 8.8 times the nominal current (Motor nominal current is 42 A) and is higher than 2.3 times the machine characteristic current ($\lambda_m/L_d$). Assuming the nominal amplitude of the initial current, the worst case is with the q-axis current only, that is, $I_{q0}= I_N$ and then $I_{d0} = 0$. In this case, the ideal ellipse exhibits the largest area, and the minimum d-axis current becomes:

$$I_{d\min} = \frac{-l_m - \sqrt{l_m^2 + \left(L_q I_N\right)^2}}{L_d} \tag{5}$$

Reaching $I_{dmin}$ = −486.36 A in the considered simulation.

Table 3. Motor parameters

| | |
|---|---|
| Voltage | $V_N = 12$ v |
| Current | $I_N = 42$ A |
| Speed | $w_N = 1245$ RPM |
| Torque | $T_N = 3.7$ N.m |
| d-axis Inductance | $L_d = 0.071$ mH |
| q-axis Inductance | $L_q = 0.25$ mH |
| Resistance | $R_s = 0.1\ \Omega$ |
| PM flux linkage | $l_m = 25$ mWb |

## 4 Minimizing braking torque

Motor torque can be expressed as the following equation:

$$T_e = \frac{3}{2}\cdot\frac{P}{2}\cdot\left(l_d i_q - l_q i_d\right) \tag{6}$$

Using equation (3) and the *d* and *q*-axis flux linkages the steady-state motor torque in short circuit mode (braking torque) results in:

$$T_{brk} = \frac{3}{2}\cdot\frac{P}{2}\cdot\left(R_s\, l_m^2 w\right)\cdot\frac{R_s^2 + \left(wL_q\right)^2}{\left(R_s^2 + w^2 L_d L_q\right)^2} \tag{7}$$

The amplitude of short-circuit current is obtained by (3), resulting in:

$$I_{sc} = \frac{\sqrt{\left(w^2 L_q\, l_m\right)^2 + \left(wR_s\, l_m\right)^2}}{R_s^2 + w^2 L_d L_q} \tag{8}$$

A typical behavior of the braking torque (negative with the motoring convention) and the short-circuit current are shown in Fig. 4 and Fig. 5 as a function of motor speed. It is possible to verify that the short-circuit current always increases with the speed $\omega$, approaching $\lambda_m/L_d$. It is worth noticing that an inappropriate choice of the motor may cause a braking torque even higher than the rated torque. Its maximum is twice the rated torque, with the IPM motor data reported in table 2.

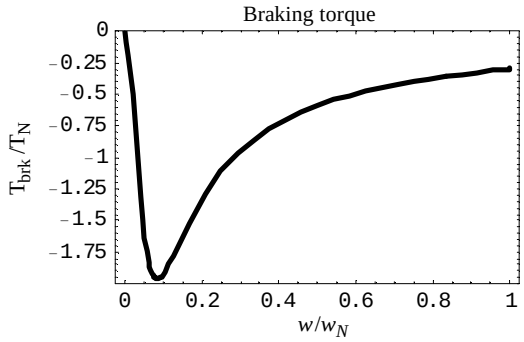


Fig. 4. Motor braking torque

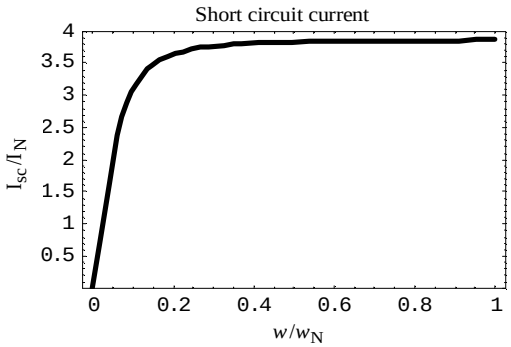


Fig. 5. Short circuit current

The maximum value of braking torque is obtained by equating the derivative of (7) with respect to speed to zero. It results in:

$$T_{brk\max} = \frac{3}{2}\cdot\frac{P}{2}\cdot\frac{l_m^2}{L_q}\cdot\sqrt{b}\cdot\frac{1+b}{\left(1+\frac{L_d\, b}{L_q}\right)^2} \tag{9}$$

Where $\beta$ is defined by following equation:

$$b = 0.5\left[3\frac{L_q}{L_d} - 3 + \sqrt{9\left(\frac{L_q}{L_d}\right)^2 - 14\frac{L_q}{L_d} + 9}\right] \tag{10}$$

It is worth noticing that the maximum braking torque is the function of $\lambda_m$, $L_q$ and $L_d$. d- and q-axis reactances are derived in terms of the reluctance ratio and the leakage flux ratios and machine dimensions of an IPM motor [5]. So with minimizing the braking torque, motor dimensions and PM flux linkage are obtained.

## 5 Motor design and optimization

The motor characteristics must satisfy the basic operating point. It means that motor perform nominal torque $T_N$=3.7 N.m at nominal speed $\omega_N$=1245 RPM while motor fed by inverter with 12V dc link. Also motor must have capability of flux weakening operation. In this case of study, a constant 500W power region is required up to a flux

weakening speed $\omega_{FW} = 3\omega_N$. Finally the motor braking torque must restrict up to 0.1 $T_N$. Thus, the design of the IPM motor has to be bound to the constraints above. The saliency ratio is supposed to be between 2 to 6, according to the adopted configuration of the rotor with one, two, or more flux barriers per pole. Also motor external dimension must satisfy EPS mechanical requirements.

In this paper, the design objectives are a decrease in motor braking torque so hat its value restricted up to 10% rated torque, an increase in motor torque and a reduction in PM volume in order to take into account the most important factors improving the motor performance and cost [6]. The torque of an IPM motor depends on the *d*- and *q*-axis inductances and the PM flux linkage, $L_d$ , $L_q$ and $\lambda_m$, respectively. These parameters depend on the dimensions and location of PM pole inside the rotor. Therefore, Magnet length, Magnet width, Outer flux barrier height and magnet pole arc are regarded as the variables to be optimized; where the latter two determine explicitly the magnet location.

The objective function, *J*, and the design constrains are presented by following equation:

$$J = \frac{m}{A}\cdot T_e + \frac{n}{A}\cdot\frac{1}{V_{PM}} + \frac{k}{A}\cdot\frac{1}{T_{brk}} \qquad (11)$$

Where $A=m+n+k$, $T_e$ is motor electric torque, $V_{PM}$ is magnet volume and $T_{brk}$ is motor braking torque. *d*- and *q*-axis inductances are reported as a function of optimization parameters in [5]. The objective function of (11) is particularly effective since its maximization results in an increase in motor torque and a decrease in PM volume and braking torque simultaneously. The relative importance of an increase in torque, $T_e$, and a decrease in PM volume, $V_{PM}$, and braking torque, $T_{brk}$, in the design is decided by desired values of *m*, *n* and *k*, respectively. In this paper the Simulated Annealing Method (SA) is used in optimization part. The SA algorithm mainly consists of repeating a sequence of iterations [8]. Given an optimization problem, at a selected initial temperature, the SA starts off with the initial solutions: current and trial, randomly selected from two points within the search space. Two energy level sets of current solution and trial solution, $E_i$ and $E_j$ respectively, are obtained. The Metropolis algorithm, generation and acceptance are then applied. If $E_i - E_j < 0$, then the trial solution is accepted and replaces the current solution. Otherwise, the acceptance or rejection is based on Boltzmann's probability acceptance, which is $PA = \exp\left(-\frac{E_i - E_j}{KT}\right)$ where $T$ denotes the temperature, k is Boltzmann's constant. If *PA* is higher than R, where R is a random value (0-1), the trial solution is accepted and replaces the current solution. If *PA* is less than R then the current solution remains and a new trial solution is generated. The generation mechanism and acceptance criterion are then repeated. After a certain amount of iterations, the temperature is reduced by multiplying its value by a factor slightly below one. With reduced temperature, these two processes are repeated again until the criterion of execution is achieved [8]. The final machine parameters and dimensions after optimization with this method are used to motor finite element simulation.

Comparing these optimization results with the specifications of a typical motor designed for EPS application shows that the design optimization results in a longer and thinner PM which is closer to the rotor surface. Table 4 compares the motor parameters, torque and PM volume of two designs. It can be seen that the optimization reduces the PM volume by 32.6% and increases the torque by 25.8%. Also the maximum motor braking torque in this case is equal to 0.23 N.m (Fig. 6). This provides major advantages for the optimized motor over the typical motor in terms of initial cost and performance, where the fault tolerance capability of motor is obtained.

Table 4. Motor characteristics after optimization

| | Initial design | Optimized design |
|---|---|---|
| Motor torque (N.m) | 3.1 | 3.88 |
| Magnet volume ($mm^2$) | 253.6 | 170.9 |
| Maximum Braking torque (N.m) | 7.03 | 0.23 |
| $L_q/L_d$ | 4.2 | 3.5 |

# 6 Finite element simulation

A motor analysis is performed by FEM to evaluate the accuracy of the relations and the optimization results obtained based on the presented model.

According to the design and optimization results, a motor schematic has been simulated in Maxwell 2D finite element software. The obtained braking torque at different motor speed is reported in Fig.6. This confirms the analytical prediction and optimization. As it seen in figure the maximum braking torque is nearly 0.23 N.m that satisfies braking torque constraint in optimization process.

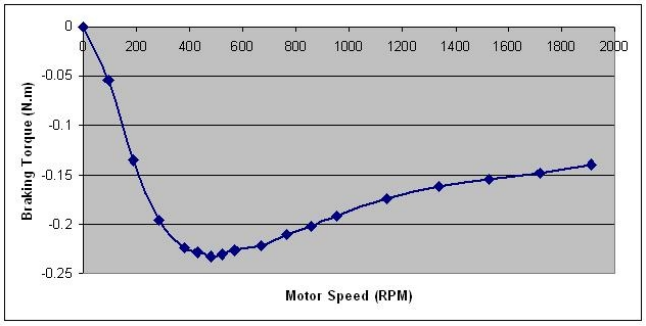


Fig.6. Braking torque obtained from FEM analysis

Fig.7 shows motor torque versus rotor initial position. First rotor rotates from zero position to 180° position by step of 2°, and then motor torque is calculated by FEM software. As it seen in the figure the maximum motor torque is increased from 3.1 N.m to 3.9 N.m because the torque density of motor is one of the objectives of optimization process.

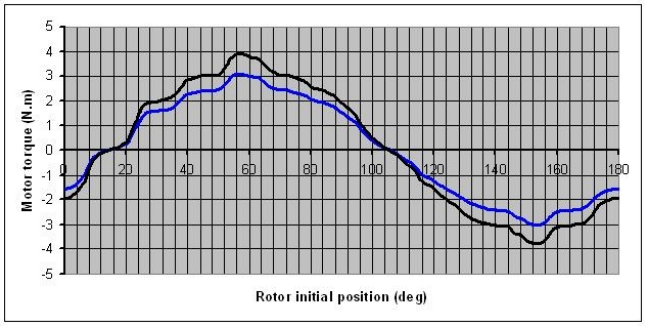


Fig.7. Motor torque versus rotor position

In Table 5, analytically obtained *d*- and *q*-axis inductances are compared with ones obtained using FEM.

Table5. Motor inductances

| | Analytical relation | FEM |
|---|---|---|
| $L_d$ *(mH)* | 0.088 | 0.071 |
| $L_q$ *(mH)* | 0.37 | 0.25 |

## 7 Conclusion

In this paper the specifications required by electric power steering application are discussed, and the IPM motor has been designed and optimized to be a promising solution. The three-phase short-circuit fault is considered to be the worst case for fault tolerance capability study. This fault has been analyzed in detail for braking torque and short circuit current. The maximum braking torque and short-circuit current are computed during transient and steady-state conditions. The procedure for the choice of the motor parameters is illustrated. Useful relationships between the maximum braking torque and the motor parameters are found and used in the motor design.

A design optimization is performed on an IPM motor in search for proper PM poles dimensions and locations to achieve a reduced magnet volume and a high developed torque. The design optimization leads to an IPM motor with more than 32.6% reduction in PM volume and 25.8% increase in the developed torque with respect to the initial design. The IPM motor designed by the proposed optimization method is analyzed by FEM to evaluate and confirm the accuracy of the machine model employed in the design and the optimization results.

*References:*

[1] M.Blanke, J.S. Thomsen, Electrical steering of vehicles fault tolerant analysis and design, *Microelectronics Reliability*, (2006) 1421–1432.

[2] Y. Liao ,H. Du, Modeling and analysis of electric power steering system and its effect on vehicle dynamic behavior, *International Journal of Vehicle Automotive System*, Vol. 1, No. 2, pp. 153-166, 2003.

[3] D.Hyeok, H.Kyo, D.Joon, Multi objective optimal design of interior permanent magnet synchronous motors considering improved core formula, *IEEE Transaction on Energy Conversion*, (1999) 1347–1352.

[4] N.Bianchi, M.Dai Pré, S.Bolognani, Design of a Fault-Tolerant IPM Motor for Electric Power Steering, *IEEE Transactions on vehicular technology*, VOL. 55, NO. 4, July 2006.

[5] C.C. Hwang, S.M. Chang, C.T. Pan, T.Y. Chang, Estimation of parameters of interior permanent magnet synchronous motors, *Journal of Magnetism and Magnetic Materials*. (2002) 600–603.

[6] S.Vaez-Zadeh, A.R.Ghasemi, Design optimization of permanent magnet synchronous motors for high torque capability and low magnet volume, *Electric Power Systems Research*. (2005) 307– 313.

[7] T. Ohnishi, N. Takahashi, Optimal design of efficient IPM motor using finite element method, *IEEE Transaction on Magnetics*, (2000) 3537–3539.

[8] L.Ingber, Simulated annealing: practice versus theory, *Mathematical and Computer Modeling*, vol.18, pp.29-57, 1993.